HortScience 61(9):1925–1934. 2026. https://doi.org/10.21273/HORTSCI19524-26

Robust Growth, Leaf Coloration, and Adaptation of a Transgenic Purple-leaved Poplar

Steven H. Strauss, Amanda L. Garms, Cory G. Garms, Chaney M. Hart, Cathleen Ma, Zachary Heinhold, Greg Goralogia, Megan McEldowney, and Parker Wheeler
Department of Forest Ecosystems and Society, Oregon State University, Corvallis, OR 97331, USA

Laurence Schimleck
Department of Wood Science and Engineering, Oregon State University, Corvallis, OR 97331, USA

Ximin An
Beijing Forestry University, Beijing, China

Keywords. anthocyanin, ecophysiology, GMO, hyperspectral, instability, ornamental, remote sensing

Abstract. **We studied leaf pigmentation, and several aspects of tree growth and physiology, in transgenic purple and wild-type trees in the field with the goal of evaluating leaf color and stability of color expression, and general growth and adaptation in a natural environment over several years. The transgenic trees overexpressed a *MYB* transcription factor gene that regulates anthocyanin biosynthesis. Thirty-six transgenic insertion lines made within the model poplar hybrid *Populus tremula* × *alba*, along with a green wild-type control of the same clone, were grown in western Oregon for three growing seasons. The color intensity and quality of purple leaf color varied widely between transgenics made with the *MYB transcription factor* from poplar (*Ptr MYB119*) overexpressed under the cauliflower mosaic virus double-35S promoter vs. that from grape (*Vv MYBA1*) that was overexpressed under the same promoter. The grape-derived *MYB* transgenics had far darker leaves than the poplar-derived *MYB* transgenics or controls, and had distinctive colorimetric, spectral, and hyperspectral profiles from laboratory and remote sensing measurements. They also had much slower growth, less efficient leaf photosynthetic parameters, and higher mortality. The grape-gene transgenics also showed a higher degree of leaf mottling and instability of leaf coloration within and between insertion events. In contrast, the poplar-gene transgenics, although having distinctly purple leaves, had growth and survival that was nearly the same as in the controls. The poplar gene–derived purple transgenics appear very well suited for use as an ornamental in temperate environments.**

Introduction

Anthocyanins are a diverse group of flavonoid pigments that are thought to provide nutritional benefits and aid in tolerance of stress in living plants (Cappellini et al. 2021; Fang et al. 2019; Zhao and Tao 2015). They are also of high value in ornamental plants, as they can brighten and diversify the colors of flowers, fruits, leaves, and stems. Natural or induced mutants that alter leaf, fruit, or flower pigmentation by modification of anthocyanin composition and levels are widely known and have been extensively used in ornamental crops. Because the genes that modify anthocyanin biosynthesis are becoming well known, and biotechnology-based methods for genetic modification of ornamental plants are improving, there is an opportunity for the rapid, directed modification of colors to help diversify plantings (Okitsu et al. 2018).

The most common transgenic approach for modification of organ color has been to overexpress natural positive regulators of biosynthetic activity, using strong promoters such as that of the widely used cauliflower mosaic virus. This was the method used to create the much-publicized purple tomato, now eligible for commercial use in the United States (Martin and Butelli 2024). Building on earlier studies that established the effectiveness of genes employed in the woody plants *Citrus* and *Populus* (Cho et al. 2016; Dutt et al. 2016), we created transgenic trees with the goal of studying their pigmentation and growth phenotypes in a temperate field environment over several natural growth cycles. In the outdoors, plants are subject to multiple seasonal cycles of temperature and moisture stress—which may affect pigmentation, growth, and survival.

Evaluating the stability and performance of novel tree phenotypes under field conditions presents a significant challenge. Traditional phenotyping often relies on slow, laborious, and sometimes destructive measurements. To improve phenotypic evaluations, we also employed a high-throughput, nondestructive proxy—Unmanned Aircraft System (UAS)-based remote sensing. This may help to ensure rapid, repeatable performance evaluation.

The objective of the study was to evaluate leaf color and stability of color expression, and general growth and adaptation, in a natural environment over several years. We report that although one of the transgenes studied caused extremely attractive, dark purple foliage, it was also highly deleterious to growth and survival. However, the other construct studied gave rise to an attractive purple phenotype that was stable over years in most transgenic lines and had almost no measurable negative impacts on tree health. It appears suitable for use in transformation of ornamental plants in temperate environments, where it should help to beautify to homes and local landscapes.

Materials and Methods

Plasmid construction. Construct Pc2300-V-V-Myb (*Vitis vinifera* MYBA1 gene; Dutt et al. 2016) was provided by Dr. Manjul Dutt at the University of Florida. Construct 35S::Ptr MYB119, with the *Populus trichocarpa* MYB119 gene; Cho et al. 2016), was provided by Jin-Seong Cho in the Kyungpook National University of the Republic of Korea. Both constructs had a double-35S gene driving *MYB* gene overexpression.

Plant transformation. Poplar clone 717-1B4 was transformed using *Agrobacterium tumefaciens* (strain *AGL1*) based on the protocol described by Filichkin et al. (2006). Briefly, leaf and stem explants were selected on callus induction, shoot induction, shoot elongation, and rooting media using kanamycin. Rooted plants from 24 Ptr MYB119 insertion events and 12 VV MYBA1 insertion events (hereafter called "events") were obtained based on polymerase chain reaction (PCR) confirmation (band presence plus correct size in transgenic plants but not wild-type control plants) using the forward/reverse primers GCATAGTCACCACTTCAAAAAGG/TCCCTGGATTTGTTCAATCATAC [376 base pairs (bp)] for VV MYB1 and TTATTCAACAGTATCGCCACCTT/GTCCTTCAGGTTGTTGTTGATCT (308 bp) for Ptr MYB199.

Two kinds of micropropagated controls that had not been subject to transformation treatments were included in the field study. The two types had been propagated and planted at different times. "Ptmyb Control"

Received for publication 13 May 2026. Accepted for publication 22 Jun 2026.
Published online 29 Jul 2026.
We thank Professor Seri Robinson for use of the colorimeter.
S.H.S. and A.L.G. are co-senior authors; they contributed equally to this paper.
S.H.S. is the corresponding author. E-mail: Steve.Strauss@oregonstate.edu.

was propagated and planted at the same time as the transgenics but few survived. Additional controls ("control") were therefore planted in the spring of the following year; they were larger at planting due to their growth in the greenhouse over winter. The two control groups were thus differentiated during statistical analysis but merged for graphical and summary statistics.

Propagation and planting. General methods for propagation and acclimation to soil are outlined in Meilan and Ma (2006). We transplanted several rooted ramets of the PCR-verified in vitro trees into soil in Corvallis, OR, USA, in Feb 2018; the plants were placed in zip-lock bags that were gradually opened to ambient air in the head-house of a greenhouse. The plants then grew in the greenhouse for 18 months, acclimated in a lath house for nearly 3 months, and were then planted in the field in Corvallis on 1 Nov 2019 using a completely randomized design (control trees and those from all events from both constructs randomized together). Tree spacing was 2.1 m × 2.4 m (7 ft × 8 ft), with the area totaling 0.05 ha, and tags were placed on each tree for identification. Trees were not fertilized but were "singled" (minor branches trimmed to leave a single dominant stem) as trees began to grow in Summer 2020, but not trimmed thereafter (and most developed multiple main branches over time). From 2000 to 2022, trees were watered with an aboveground sprinkler system for 2 hours each Monday, Wednesday, and Friday morning; no irrigation was applied in 2023 and 2024. The sites were mowed between trees several times each year to keep weeds a manageable size. The trees (Fig. 1) were grown under permit from US Department of Agriculture Biotechnology Regulatory Services, no. 19-011-101, and then continued under 20-010-103r, 20-261-108r, AUTH-0000203519, and finally Permit #124-2E386NX.

Leaf measurements. Three leaves were collected from each tree from the tallest leader stem by finding the first fully expanded, mature leaf and then collecting the three leaves below that. Leaves were scanned using an HP Scanjet 8200 (HP, Palo Alto, CA, USA) and included a ruler; leaf area in cm^2 was calculated using ImageJ software (National Institutes of Health, Bethesda, MD, USA). Relative chlorophyll content was measured in the field using a handheld SPAD 502 Plus Chlorophyll Meter (Konica Minolta, Tokyo, Japan). Three measurements were taken and averaged on each leaf.

Physiology. Several physiological measurements were taken to assess changes in net gas exchange and light-use efficiency. Diurnal changes in stomatal conductance (g_{sw}, mmol H_2O/m^2*s), electron transport rate (ETR, μmol e^-/m^2*s), leaf temperature (T_{leaf}, °C), and Photosystem II quantum efficiency (φ_{PS2}) were measured with a handheld LI-COR-600 fluorometer/porometer (LI-COR, Lincoln, NE, USA) at 1000, 1200, 1400, and 1600 HR on a hot and dry day in late Aug 2022 (31 Aug 2022: maximum temp of 31.3 °C and maximum vapor pressure deficit (VPD) of 2.73 KPa).

Fig. 1. Images of transgenic and control trees growing in the field. (**A**) In foreground, grape construct, event 57-1; (**B**) grape construct event 7-1; (**C**) poplar construct, event 92-2; (**D**) poplar construct event 120-1 next to Dr. Greg Goralogia (1.7 m) for scale; and (**E**) controls #1 and (**F**) #5. Photos were taken in Jun 2023.

ETR was calculated as $\frac{\Phi_{PS2}*Q_{ambient}*\alpha*PS2}{PS1}$ where $Q_{ambient}$ is photosynthetically active radiation (PAR) (μmol photons/m^2*s), α is leaf absorption under actinic light (assumed to be 0.8), and $\frac{PS2}{PS1}$ is the partitioning of photons to photosystems I and II, and is assumed to be 0.5. Two-way analysis of variance (ANOVA) with construct and measurement hour (repeated measures ANOVA) was used for analysis.

On a clear date in early Fall 2022 (7 Oct 2022: maximum temperature of 24.7 °C and a maximum VPD of 1.29 KPa), a portable photosynthesis system (LI-COR-6800) was used to measure light-response curves for net photosynthesis and ETR over a spectrum of PAR. Measurements were taken on up to 3 ramets per construct. Data for each curve was fit to a nonrectangular hyperbolic model (Marshall and Biscoe 1980) using nonlinear least squares with the R package photosynthesis (Stinziano et al. 2019). Model fit was visually assessed for goodness of fit and then used to derive empirical parameters including A_{sat}, the asymptotic level of carbon assimilation (A_{net}) with increasing PAR, quantum yield (φ_J: slope; increase in A_{net} per unit increase in PAR within the linear portion of the model), and light compensation point (x-intercept: the PAR level at which carbon assimilation balances loss from respiration).

Growth measurements. We measured several tree and leaf variables over several years, including stem basal diameter (at 150 mm height), and total length of the tallest stem or branch. There were a total of 11 control, 16 grape construct, and 18 poplar construct trees for most analyses. From height and diameter we calculated volume index (diameter squared × height) as an indication of relative biomass growth. Tree survival was scored, along with evidence of winter frost damage based on spring growth (no evidence of damage was seen in any trees, thus data are not presented). Trees that did not flush leaves were scored as dead. Branch length for all major branches 4 inches or longer was collected in Summer 2021 and used to calculate "branchiness" [(standard deviation of branch length)/(mean branch length) × 100] and cumulative branch length (sum of longest seven branch lengths per tree).

Leaf color intensity and stability. We used a Konica Minolta CR-5 colorimeter employing the CIE2000 *L*a*b** color space (CIELAB 2025), where *b** indicates blue-yellow color and a* indicates green-red color; measurements were taken on leaves that had been collected in the field the day of measurement. Readings (30 mm) were taken for both the adaxial and abaxial sides of the leaves and averaged. A chroma plate was measured daily to calibrate the colorimeter. We visually scored color intensity, uniformity, and leaf mottling (Fig. 2) in the field using three heuristic indexes. For system I scored in 2020: The scoring scale for a whole tree was 1 through 4, with 1 being green (no purple at all), 2 and 3 being progressive intermediates, and 4 being the most dark purple (Fig. 3D).

Hyperspectral imaging of individual leaves. Hyperspectral images of field-collected leaves were recorded over 397 to 1004 nm at a spectral resolution of 1.35 nm, using a Specim FX10 camera (Specim, Spectral Imaging Ltd., Oulu, Finland). Tungsten halogen lamps illuminated the samples, and sample motion and image acquisition (which included a dark current and white reference before collecting individual images) were controlled using Lumo software supplied with the system. Samples were analyzed on a black background and care was taken to minimize exposure time to the intense light of the lamps (less than 1 minute).

Fig. 2. Examples of between-construct, within-tree, and within-leaf variation in coloration. (**A**) Bilateral variation and (**B**) asymmetric variation in leaf color from a grape construct tree, event 59-4, and (**C**) bilateral and (**D**) developmental variation in color in a grape construct tree, event 60-3. (**E**) Side-by-side comparisons of representative, nonmottled leaf samples from each construct, photographed indoors: control 2, poplar 124-4, and grape 59-5 (from left to right). (**F**) Variation between branches within a single tree of grape construct 60-3. Photos were taken during the 2021 growing season.

An individual image was obtained from three leaves per clone, with relative reflectance values calibrated for each image with the corresponding dark current and white reference data. Regions of interest, corresponding to each of the three leaf samples analyzed per clone, were identified and cropped using MATLAB (MathWorks, Natick, MA, USA) to give individual spectra. Spectra were later averaged to give an individual spectrum per tree that was used in subsequent analysis.

Quantitative analysis. We used RStudio (Boston, MA, USA) version 2023.06.2 + 561 "Mountain Hydrangea" for most analyses. ANOVA mixed models using Type III sums of squares were employed where construct was a fixed effect and event was a random effect, implemented by the RStudio package lmerTest combined with lme4. Post hoc analyses included RStudio Tukey tests using estimated marginal means, and Emmeans for pairwise contrast analysis.

Principal components analysis (PCA) was used to reduce dimensionality of several groups of data, including for growth, colorimeter, and hyperspectral data. For hyperspectral leaf analyses, a model was developed using Unscrambler (version 9.2) software (Camo AS, Oslo, Norway). PCA compressed the spectral information from wavelengths in the range 397 to 1004 nm into much fewer dimensions that captured maximum variance per dimension. PCA score plots of leaves from individual clones were used to examine overall similarities of events and constructs. To increase discrimination, subsequent analysis using 397 to 700 nm and spectra transformed using a second derivative from 480 to 600 nm was used to more clearly discriminate constructs.

Remote sensing. We employed a UAS [DJI Matrice M300 (Shenzhen, China)] operating with a real-time kinematic (RTK) base station and active RTK positioning. Light detection and ranging (LiDAR) data were collected on 14 Jul 2023 using a DJI Zenmuse L1 sensor to generate horizontal profiles of trees in the field, from which crown area measurements were derived. On 28 Aug 2022, thermal profiles and multispectral data alongside RGB images were collected for individual trees using a DJI Zenmuse XT2 thermal camera and a Micasense RedEdge-MX

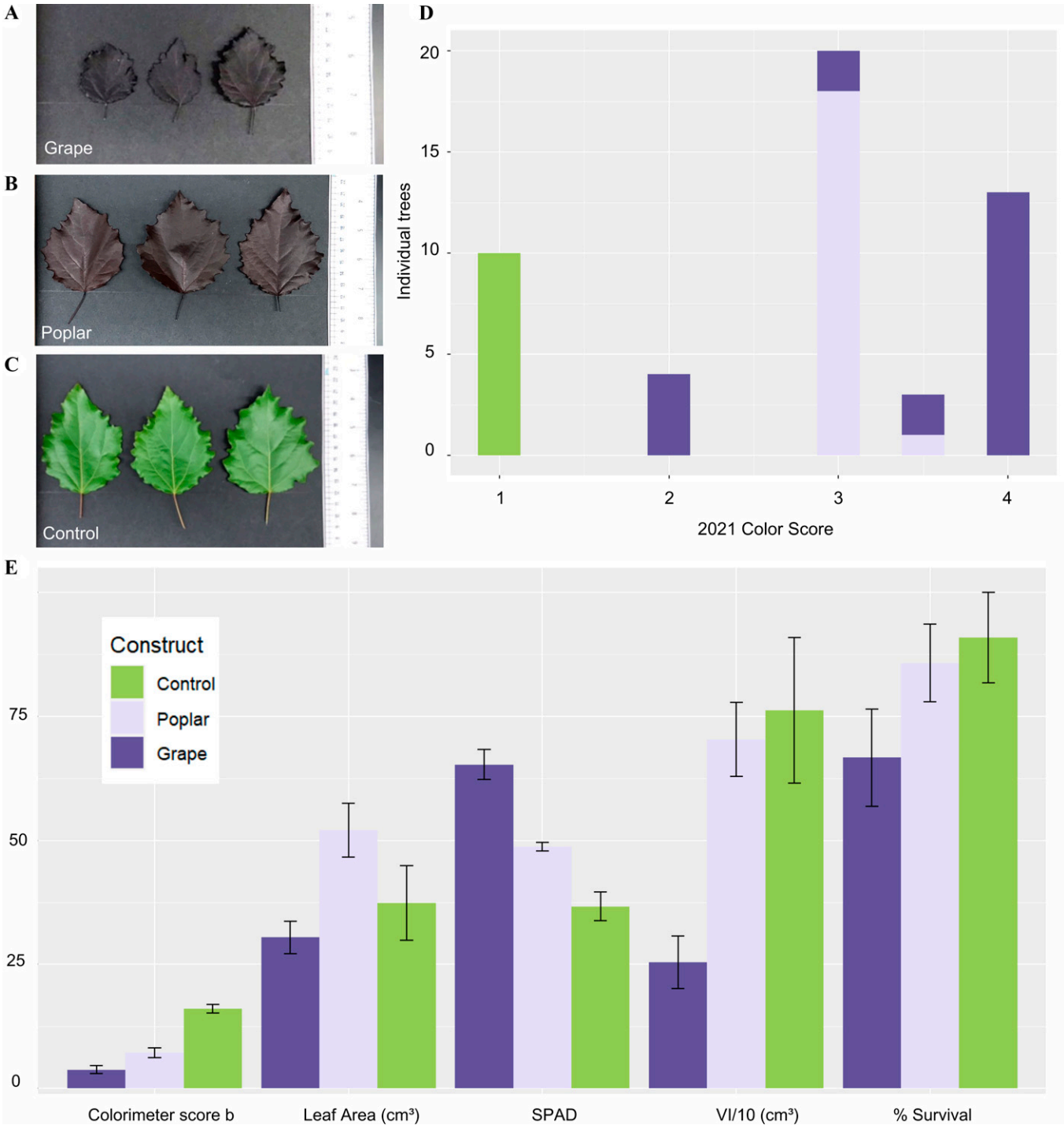

Fig. 3. Summary of leaf color and growth characteristics among constructs. (**A–C**) Three representative leaves on a black background similar to that used for hyperspectral analyses (**A,** grape construct event 84-1; **B,** poplar construct event 120-1, and **C,** wild-type control). (**D** and **E**) Construct type is denoted by colors (green = wild-type control, light purple = poplar construct, dark purple = grape construct), also shown in the legend in (**E**). In (**D**), predominant leaf color for trees was subjectively scored in the field on a 1 to 4 scale (1 is green with no purple coloring, 2 is very light/mottled purple, 3 is moderate and consistent purple as was common for the poplar construct, and 4 is consistently dark purple as was common for the grape construct). (**E**) Histogram of construct values and ± 1 standard error for several traits. From left to right: Colorimeter score b determined in the laboratory from field grown leaves; mean single-leaf area (cm^3), SPAD chlorophyll index, volume index of the trunk (VI 10), and survival as of Summer 2023. All living trees at the time, nine controls, 24 grape, and 21 poplar construct trees, were scored.

multispectral sensor (Wichita, KS, USA), respectively. For the multispectral flights, standard radiometric calibration panels were used before and after flights, and correction was performed using the empirical line method. To address the challenge of processing proprietary radiometric JPGs from the thermal sensor, a custom workflow (available at https://github.com/cory-garms/thermal_conversion_demo) was developed using thermal_parser and exiftool to convert images to functional rasters (.tif), with re-appended GPS metadata. Radiometric metadata were retrieved from a local weather station (National Weather Service 2026) when possible and standardized across the flights to ensure consistent relative temperature profiles. A variety of vegetation indices were derived from these data (Supplemental Table 1). Indexes included were Anthocyanin reflectance index (ARI); Excess Green Index (EXG); Excess green minus Excess red index

(EXGR); Green Chlorophyll Index (GCI); Green Red Vegetation Index (GRVI); Green Normalized Difference Vegetation Index (GNDVI); Near Infrared (NIR); Normalized Difference Vegetation Index (NDVI); Modified Green Red Vegetation Index (MGRVI); Modified Soil Adjusted Vegetation Index (MSAVI); Normalized Difference Red Edge (NDRE); soil-adjusted vegetation index (OSAVI); Red edge band from multi spectral sensor (RE); vegetation index responsive to chlorophyll (RECI); Soil Adjusted Vegetation Index (SAVI); Thermal Infrared (TIR); and Triangular Greeness Index (TGI). Further details about remote sensing procedures and downstream data analysis are provided in Supplemental Methods File 1.

Results and Discussion

We present a multiyear field study of the effects of two *MYB* transcription factor overexpression constructs on the growth and development of a poplar clone. We recorded a variety of growth, physiology, and color data to help evaluate the potential of these kinds of transgenic trees as ornamental varieties.

Color traits. The foliage from trees produced with the two constructs were strikingly different from each other and from the controls. The differences were obvious in the field (Fig. 1) but also easily seen on leaves imaged in the laboratory, where nearly all trees containing the grape construct had much darker foliage than those with the poplar construct (Fig. 3A–C). There was little overlap between the visual color scores from the grape and purple poplars; nearly all could be distinctly recognized in the field based on leaf color (Fig. 3D).

Colorimeter measurements of leaves from trees with the grape construct vs. the poplar construct differed significantly from that of the control trees on both the *a** and *b** axes, showing a change in the green-red axis and blue-yellow axis, respectively; the differences between constructs and control trees from ANOVA were highly statistically different, as was the brightness dimension *L* (Table 1, Supplemental Table 1B). These scores indicate that their measured coloration is both bluer and redder than the control leaves, which is consistent with the observed purple coloration. The difference from control was especially evident in the *b** dimension (blue-yellow), with clearly nonoverlapping standard error bars distinguishing the constructs and controls (Fig. 3E). Tukey tests showed that ANOVA differences were primarily due to the differences between the two constructs vs. controls; the grape vs. poplar construct contrasts were significantly different only for the "brightness" parameters, L and SPAD (Supplemental Table 1A). This is likely to be a result of the darker purple color of the grape construct leaves compared with control. The colorimetric differences can also be seen from PCA of the three colorimeter dimensions, where PC1 (87% variance explained) best distinguished controls from trees with the two transgenic constructs, and PC2 (11% variance explained) best discriminated trees with the grape vs. the purple construct; both PCs were statistically significant by ANOVA (Table 1, Fig. 4, Supplemental Table 1B).

Table 1. Summary of ANOVA *P* values for differences among construct and control groups, standard errors (*SE*), and percentage differences in means of selected traits. Percent values are relative to controls, set at zero. *P* values less than 0.05 are shown in bold. Physiology variables, g_{sw}, φ_{PS2}, ETR, and T_{leaf}, are for the 1400 HR time point on a hot day in Aug 2022. Physiology variables, A_{sat}, quantum yield (φ_J), and light compensation point (LCP) are from a milder day in early Oct 2022.

	Construct	Means	*SE*	% difference	*P* value
Physiology variables					
g_{sw}	Control	0.430	0.029	0.00	**<0.001**
(stomatal conductance)	Grape	0.203	0.020	−52.86	
	Poplar	0.261	0.022	−39.30	
φ_{PS2}	Control	0.493	0.026	0.00	**<0.001**
(maximum fluorescence yield)	Grape	0.516	0.018	4.73	
	Poplar	0.527	0.020	6.80	
ETR	Control	287	21.2	0.00	**0.02**
(electron transport rate)	Grape	316	14.7	10.34	
	Poplar	351	16.2	22.30	
Tleaf	Control	32.036	0.311	0.00	**<0.001**
(leaf temperature)	Grape	33.799	0.215	5.50	
	Poplar	33.563	0.237	4.77	
A_{sat}	Control	21.8	2.58	0.00	0.238
(net assimilation at light saturation)	Grape	14.8	2.58	−32.02	
	Poplar	18.7	2.58	−14.36	
Quantum yield (φJ)	Control	0.0479	0.004	0.00	**0.043**
	Grape	0.0286	0.004	−40.28	
	Poplar	0.0348	0.004	−27.47	
Light compensation point (LCP)	Control	42.2	8.63	0.00	0.200
	Grape	66.8	8.63	58.32	
	Poplar	49.6	8.63	17.58	
Coloration variables					
PC1 (397–1004 nm, hyperspectral)	Control	0.044	0.004	0.00	**0.011**
	Grape	−0.016	0.008	−135.63	
	Poplar	0.004	0.005	−90.09	
PC2 (397–1004 nm, hyperspectral)	Control	−0.020	0.007	0.00	**0.037**
	Grape	−0.001	0.004	−95.27	
	Poplar	0.017	0.008	−182.20	
SPAD ′22	Control	36.670	2.861	0.00	**0.001**
	Grape	65.281	2.979	78.02	
	Poplar	48.713	0.908	32.84	
Colorimeter score b*	Control	16.072	0.887	0.00	**<0.001**
	Grape	3.743	0.780	−329.37	
	Poplar	7.171	0.978	−124.13	0.001
Survival, growth, and morphology variables					
Mean leaf area	Control	37.343	7.524	0.00	0.057
	Grape	30.417	3.265	−18.55	
	Poplar	52.055	5.421	39.39	
Volume index 2023	Control	76.241	14.651	0.00	**0.013**
	Grape	25.407	5.261	−66.68	
	Poplar	70.327	7.479	−7.76	
Percent survival	Control	90.909	9.091	0.00	χ^2 *P* value
	Grape	66.667	9.829	−26.67	**$1.3E^{-05}$**
	Poplar	85.714	7.825	−5.71	
Remote sensing variables					
Projected crown area	Control	0.892	0.160	0.00	**0.01**
	Grape	0.397	0.059	−55.47	
	Poplar	0.829	0.079	−7.06	
Normalized difference vegetation index mean	Control	0.511	0.018	0.00	**0.001**
	Grape	0.362	0.020	−29.16	
	Poplar	0.519	0.021	1.57	
Anthocyanin reflectance index mean	Control	1.619	0.145	0.00	**<0.001**
	Grape	1.919	0.147	18.53	
	Poplar	3.196	0.187	97.41	

Instability or chimerism in coloration was common in trees from several events, where parts of leaves or entire branches lacked color although nearby leaves and branches were uniformly purple (Fig. 2A–D, F). In the field, instability of transgene expression was also observed as leaf mottling across leaves and branches, and it was seen more frequently in trees containing the grape construct vs. those with the poplar construct. There was substantial mottling in two of eight events (25%) in trees with the grape construct vs. one of seven events (14%) seen in trees with the poplar construct (scored in 2022). Four trees were notably mottled or variable in color within trees from the grape event (as observed in 2001: Fig. 3D, score category 2). These unstable transgenic events exhibited inconsistent color development across multiple growing seasons and could therefore be easily identified and excluded as candidates for potential variety development. Differences in color stability

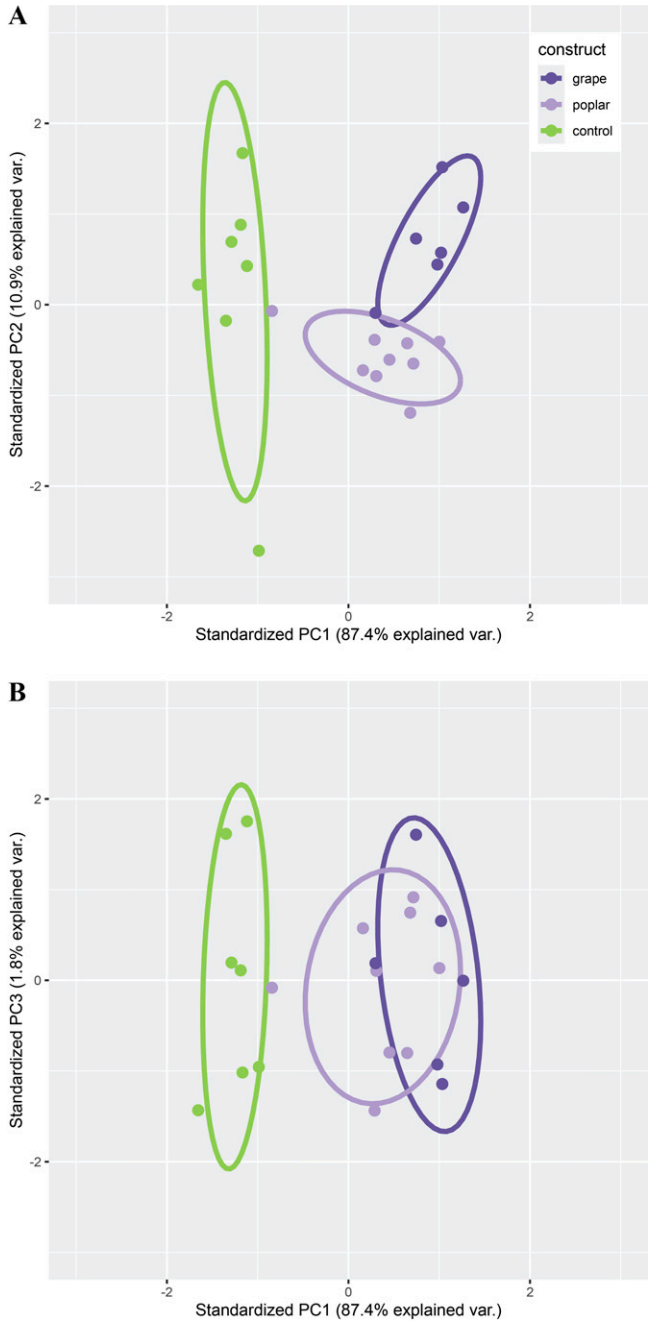

Fig. 4. Principal components analysis plots based on three-dimensional colorimeter scores. PC1 accounted for the large majority of variance (87%) and most effectively separated control vs. transgenic trees, whereas PC2 accounted for only 11% of variance but best separated the grape and purple construct transgenic trees.

between events within a construct are likely reflective of differences in genomic "quality," which may be a result of the insertion site as well as copy number or epigenetic state of transgenes (Hobbs et al. 1993). In hybrid poplar, unstable transgene expression has previously been described as the absence of the target phenotype in entire leaves or branches of transgenic trees (Kumar and Fladung 2001).

Because of the constitutive promoters employed, and our informal observation of reddish xylem in personal samples of anthocyanin-overexpressing apples (Chagné et al. 2013), we examined whether xylem might be darker in purple vs. control trees. Stem sections from a single tree per construct type and control were collected from the field in May 2023, dissected, and imaged. Very little coloration was seen in any of the samples, thus stem sections were emersed in buffers of different acidity that we suspected may enhance color differences (pH 4, 6, and 8 in 50-mL Eppendorf tubes, viewed at 1 h, 4 h, and after overnight). These treatments did not enhance color detectably, and no consistent differences were seen between samples of constructs (data not shown). Thus, efforts to produce pigmented wood are likely to need different approaches, including different promoters and possibly different pigments that are stable after xylem formation. We did notice, however, that in the field the typically light-colored bark of these poplars was slightly darkened in trees from the anthocyanin-producing constructs (imaged in 2024); however, the difference was subtle and did not persist as trees grew in girth (data not shown). A much stronger promoter, or one that is bark-specific, may be needed to significantly affect bark color for ornamental purposes.

Hyperspectral traits. Spectral signatures for leaves from the control trees differed strongly from those of the transgenic, non-mottled trees over most wavelengths measured. Using PCA, we observed differences in mean PC scores from ANOVA over 397 to 1004 nm (Table 1) that were highly significant for PC1 (0.011) and weakly significant for PC2 (0.037). Groups fell just short of significance for PC3 and PC4 (0.085 and 0.063, respectively) (Supplemental Table 1B). Subsequent analysis using 397 to 700 nm and second derivative spectra gave strong discrimination of groups (Fig. 5B); PC1, which explained 31% of the total variance in spectral data, was the main axis separating the groups, although there was considerable overlap between stable trees containing the grape vs. the poplar constructs. The control trees formed a distinctive group from all the transgenics, and mottled trees formed an intermediate group (Fig. 5B). Only PC1 was statistically significant in the ANOVA of the groups, but highly so ($P = 0.001$, Supplemental Table 1B).

The differences among groups were most prominent at ~510, 530, 554, and 577 nm (Fig. 5A). Again using second derivatives, these differences among groups were highly statistically significant based on ANOVA (Supplemental Tables 1A and 1B). This result is consistent with previous reports citing a decrease in reflectance at 550 nm for leaves with higher anthocyanin content, even when chlorophyll content remains the same (Gitelson et al. 2001). Not surprisingly, the mottled trees were intermediate between leaves from trees of the stable constructs at all wavelengths.

Hyperspectral imaging has been previously used to detect anthocyanin content in leaf tissue and provide the basis of various anthocyanin indexes, including for anthocyanin reflectance index (ARI) as presented below (Dai et al. 2023; Gu et al. 2018; Van den Berg and Perkins 2005). Gitelson et al. (2001) found a strong difference in absorption between samples with differing anthocyanin and chlorophyll contents near 550 nm, and a similar difference was observed between trees from the control and the poplar and grape constructs in this study (Fig. 5A).

Survival, growth, and leaf size traits. The rate of survival strongly and significantly varied among trees with different constructs and controls (Fig. 3E; Table 1, $P < 1.3E^{-05}$), with the dark-purple–colored trees containing the grape construct having the lowest survival, and trees with the poplar construct and controls having similar rates of survival. Tree survival was again assessed in Jan 2025, and the rates were 91% for the controls, 85% for trees containing the poplar construct, and

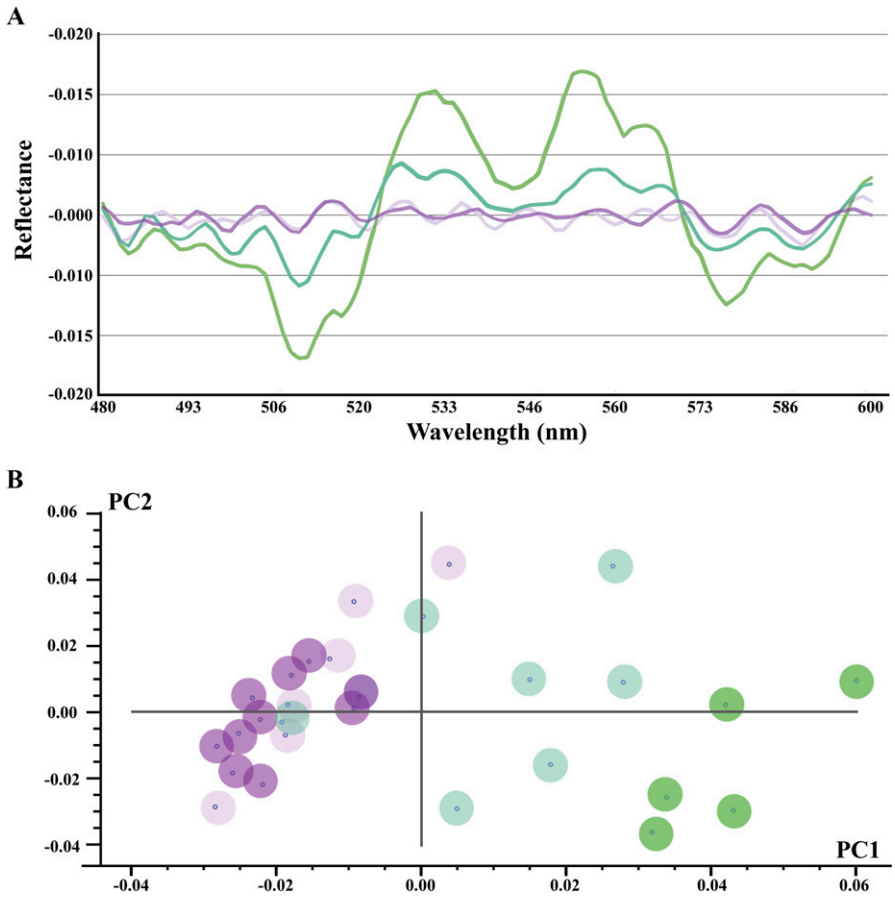

Fig. 5. Hyperspectral leaf analysis. (**A**) Reflectance for second derivative spectra. Spectra are shown for typical leaves from control (green), grape (dark purple), poplar (light purple), and mottled leaf (light green) constructs collected in the field the same day as they were scanned. (**B**) Scatterplot of PC1 (31% of variance) vs. PC2 (22% of variance) from full hyperspectral scans of leaves (397–1004 nm). Point colors are based on the color of leaves in visible light, as with panel A, bright green indicates controls, lighter green indicates mottled or variably green/purple leaves as in Fig. 2, light purple indicates the typical color of leaves from the poplar construct, and dark purple indicates the color of typical leaves from the grape construct.

58% for trees with the grape construct. The stress that led to high mortality in the grape construct may have also prompted precocious flowering (Supplemental Fig. 1); floral buds were observed during their emergence in Spring 2026 for two very small, slow-growing trees from a single insertion event (VVmybA1_83-2). However, later in the season, a fully expanded flower was also observed near the top of a large, healthy poplar construct tree that was apparently just coming into normal sexual maturity (Ptmyb_92-2_4: Supplemental Fig. 1). As a condition of our regulatory permit, all the flowers were destroyed before full expansion or seed release so the fertility of those trees could not be observed.

During in vitro transformation, the deleterious physiological effects from the grape construct may have caused it to give rise to transgenic shoots at a lower rate; the grape construct gave a rate of shoot formation under kanamycin selection that was about half that of a control construct with no *MYB* genes, whereas the rate for the poplar construct was essentially the same as for the control construct (no *MYB* genes), although these differences were not statistically significant. Unfortunately, it is impossible to draw strong conclusions as the constructs employed for the two *MYB* genes, and for a *MYB*-less green fluorescent protein (GFP) expressing "control" plasmid, were not isogenic (i.e., there were differences in the plasmids in addition to that of having different *MYB* and GFP genes; data not shown).

Tree height and volume index varied strongly and was statistically significantly in all years (e.g., Fig. 6, Table 1, Supplemental Table 1B). Trees with the grape construct had a volume index approximately two-thirds less than control trees (Table 1), whereas trees with the poplar construct were nearly the same size as control trees (reduced by ≈8%). Moreover, trees with the poplar construct did not differ significantly from control trees for any of the height, diameter, volume, or branch traits measured in any year, whereas the trees containing the grape construct were significantly different from either the control or trees with the poplar construct for nearly all size measurements (Supplemental Table 1A).

Mean single-leaf area varied among trees with different constructs, a result that was very near to statistical significance for 2023 ($P < 0.06$; Table 1, Fig. 3); poplar construct trees were nearly 40% larger than controls, and grape construct trees were nearly 20% smaller than controls. In 2021 and 2022, the differences between controls and poplar construct leaves, but not with grape construct leaves, were also statistically significant (Supplemental Table 1A). The tendency for large leaves in trees from the poplar construct, which had extensive crowns and height compared with trees in the grape construct, may result from more self-shading in the former, perhaps causing more shade-leaf–type development (which are typically larger and thinner: Kramer and Kozlowski 1979). In addition, the poor health of the grape construct may have curtailed leaf expansion. The two branchiness traits did not differ substantially or significantly between trees with different constructs or the controls (Supplemental Tables 1A and 1B), a likely result of the extensive within- and between-tree environmental variation in branching patterns.

Physiological traits. Photosynthetic efficiency was lower in transgenic trees from both constructs compared with the controls. Light-response curves showed a decrease in rate of carbon assimilation and ETR over a range of light intensities, and more so in the grape than in the poplar construct (Fig. 7A). When data from light-response curves were fitted to a model of photosynthetic response to irradiance, both constructs had lower net assimilation at light saturation (A_{sat}) and per quanta rate of carbon assimilation (quantum yield φ_J), along with a higher light compensation point (LCP) (Fig. 7B). A_{sat} and quantum yield were decreased 32% and 14%, and LCP increased 58% and 18%, in the grape and poplar construct trees relative to control, respectively (Table 1).

When measured from midmorning to late afternoon on a hot and dry date in Aug 2022, trees from both constructs showed a much reduced stomatal conductance, and increasing leaf temperature during the day, compared with controls (Fig. 7C). Toward late afternoon (1600 HR), leaf temperature for all trees became similar, likely due to increased wind at that point (Supplemental Fig. 2). The wind presumably reduced the leaf boundary layer, resulting in greater heat transfer from leaves (Daudet et al. 1999), cooling the purple leaves to a similar temperature as that of controls. Trees from both constructs demonstrated consistently higher ETR than control trees during this same period (Fig. 7C). Differences in ETR among groups was statistically significant at 1000 and 1600 HR, but not at 1200 and 1400 HR (Supplemental Table 1B). Apart from 1200 HR where grape and poplar construct trees differed from controls, this was due to differences between poplar construct and control trees (Supplemental Table 1B). This effect appeared to be driven in part by differences in incident light between sampled leaves for each construct (Supplemental Fig. 3) but also may be a result of differences in effective quantum

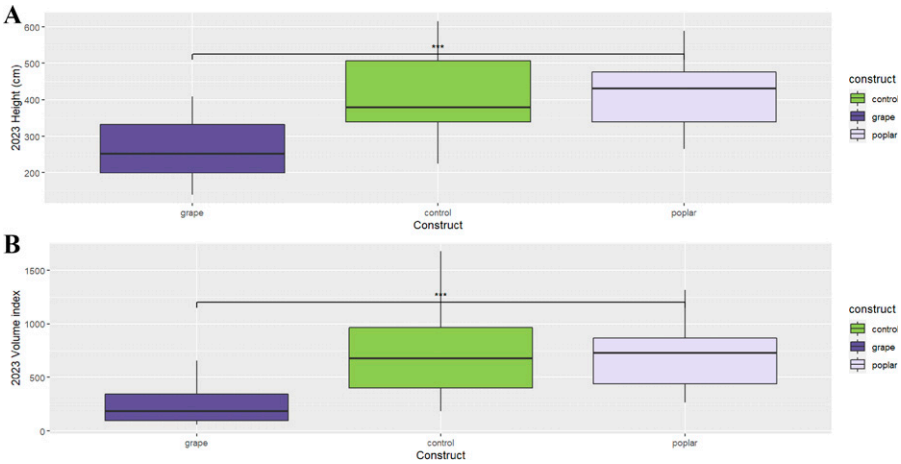

Fig. 6. Construct effects on tree stem growth. Trees with the control and poplar constructs were significantly larger in volume index (**A**) and height (**B**) than those with the grape construct, but the control and poplar constructs did not differ significantly from each other. Bars and asterisks are from Tukey contrasts, with three asterisks indicating significance at the 0.01 level between grape and either the control or poplar construct trees.

efficiency (φ_{PS2}) in the transgenic trees as compared with controls (Fig. 7C).

The increases in anthocyanin content in the transgenic trees clearly had an unfavorable effect on photosynthesis and leaf temperature, although may have provided some photoprotective benefits. The increased light absorption from the dark leaves, combined with reduced stomatal conductance and associated transpiration cooling, are likely causes of the higher leaf temperatures. Despite these negative effects, higher anthocyanin content in trees from both constructs was associated with maintenance of higher rates of effective quantum yield and concurrent increases in ETR on an exceptionally hot and dry day (Fig. 7C). (Similar increases in ETR were not observed on the cooler day from which light-response curves were measured.) Although the photoprotective role of anthocyanins is still debated (Hughes et al. 2011), these results are consistent with anthocyanins providing some photoprotective benefits under stressful environments, such as was observed in apple cultivars (Zhao et al. 2022). For the poplar construct, the increased photochemical efficiency under stressful conditions may have provided enough benefits to nearly outweigh the impacts on leaf carbon budget via reduced photosynthesis and elevated temperature.

Remote sensing traits. LiDAR data were collected to give horizontal profiles of trees in the field (Fig. 8), from which crown area measurements were derived. Trees containing the grape construct had crown areas 55% lower than control trees, whereas trees with the poplar construct had crown areas 7% lower than controls (Table 1). Thermal cameras were used on 28 Aug 2022 to collect relative temperature profiles among adjacent trees in the same flight path alongside RGB images, minimizing the impact of absolute sensor calibration errors. A variety of indexes were derived from these data, including the normalized difference vegetation index (NDVI) and various anthocyanin indexes, including ARI (Kim and van Iersel 2023). Both the NDVI and ARI indexes were

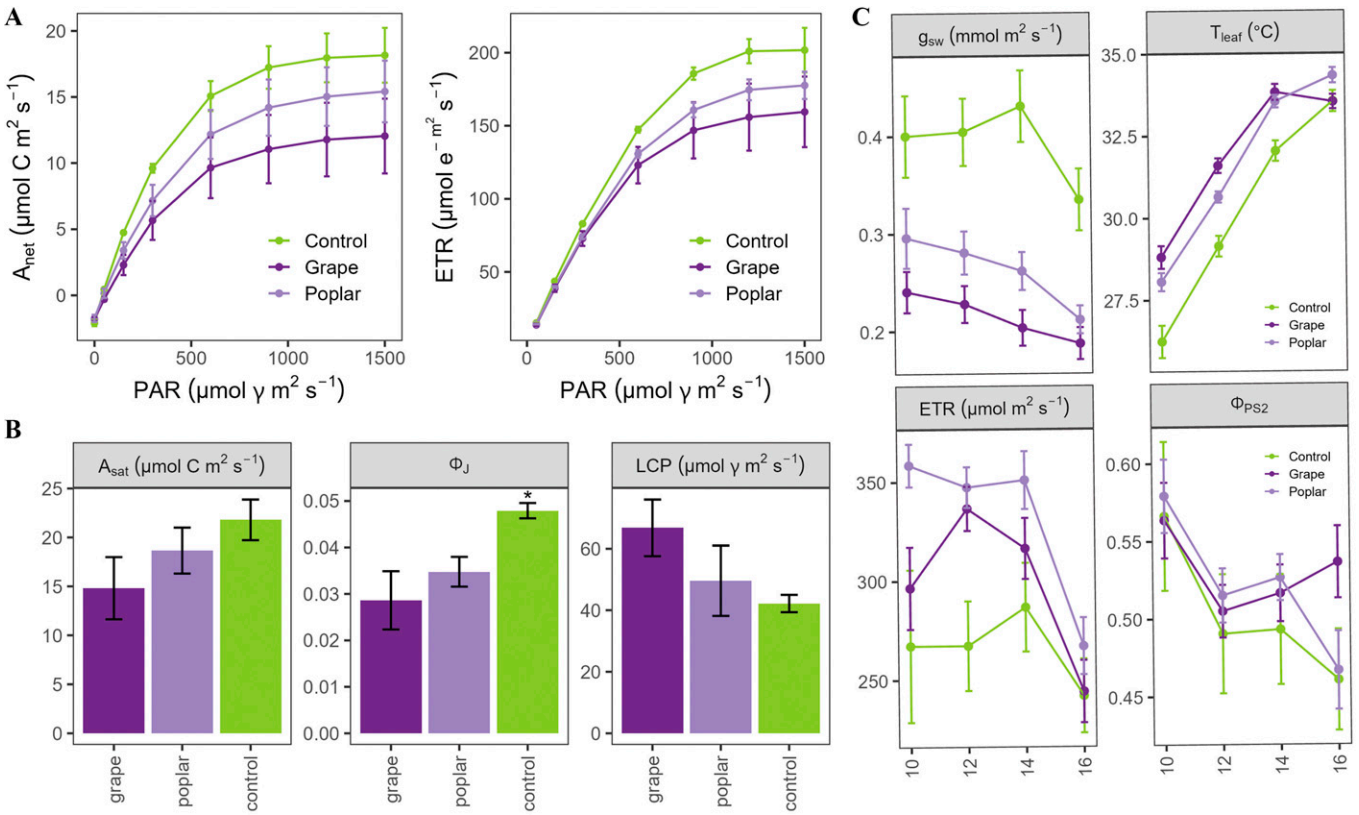

Fig. 7. Variation in photosynthesis-related leaf measurements across variable field measurement dates. (**A**) Measurements of net photosynthetic assimilation rate (A_{net} µmol·m^{-2}·s^{-1} C) and electron transport rate (ETR, µmol·m^{-2}·s^{-1}) vs. photosynthetically active radiation (PAR, photons in µmol·m^{-2}·s^{-1}) measured from light-response curves taken on a clear day in early Fall 2022 (n = 3 trees per construct with one sun leaf measured for each tree). (**B**) Differences among constructs in photosynthesis light-response parameters including A_{sat} (net assimilation at saturating light intensity), quantum yield (φ_J, maximum conversion efficiency of C assimilation per photon quanta), and light compensation point (LCP, light intensity at which C assimilation equals day-time cellular respiration) derived from model fits to nonlinear photosynthesis model (Marshall and Biscoe 1980). (**C**) Diurnal trends in stomatal conductance (g_{sw} mmol·m^{-2}·s^{-1} H_2O), leaf temperature (T_{leaf} °C), ETR and ϕ_{PS2} (effective quantum yield of photosystem II) for a hot and dry day in Aug 2022. Bars show ± 1 standard error of the mean from measurement of multiple leaves (n = 11–22).

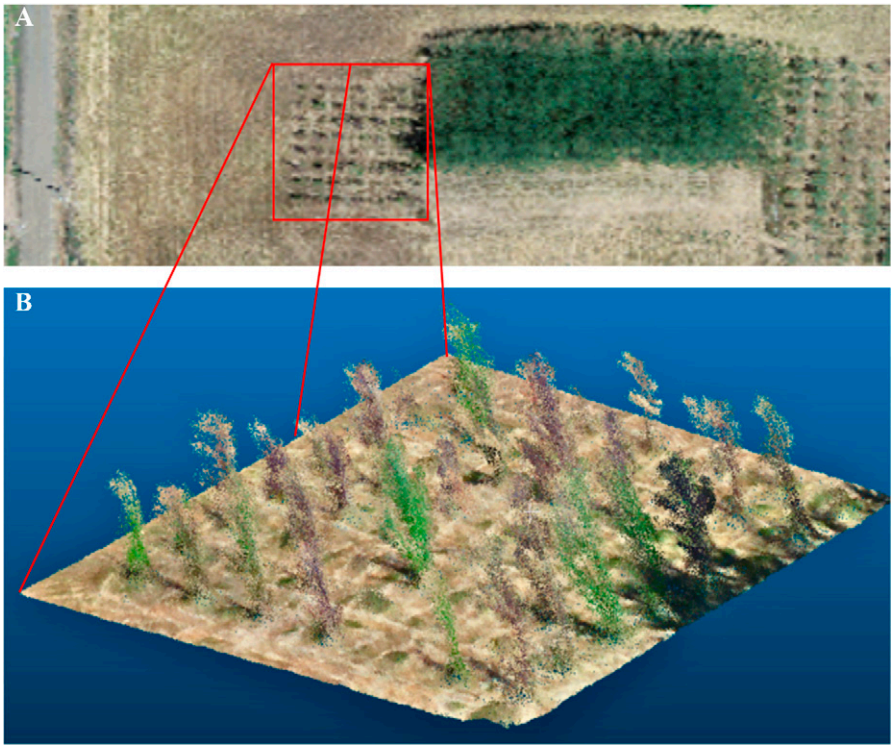

Fig. 8. Drone imaging and data analysis. (**A**) Image of the field site taken using a DJI Terra sensor in Summer 2023, georeferencing of EPSG: 26910 (NAD83/UTM Zone 10N). (**B**) Zoomed-in rendered LiDAR point clouds of the processed data using a LidR package (https://r-lidar.github.io/lidRbook/).

highly statistically differentiated between trees with different constructs and controls, with NDVI nearly 30% lower in trees containing the grape construct compared with control trees, and trees containing the poplar construct having levels essentially the same as the controls (Table 1). As expected, ARI levels were higher in the transgene-containing trees compared with the control trees, but the lighter purple–leaved trees containing the poplar construct had higher levels than did the darker leaves of trees with the grape construct (Table 1), perhaps because the darkness of leaves from trees with the grape construct gave a lower reflectance in total, or there were more green weeds imaged below their sparser, shorter canopies. These results suggest that relying solely on the ARI index to quantify pigment levels, without chemical validation, is premature; severe physiological stress or sensor saturation in the darkest leaves may skew the expected linear relationship between the index and true anthocyanin concentration.

We calculated a variety of other indexes from the drone imaging (Supplemental Table 1). Several of them relate to the "greenness" and chlorophyll content vs. interfering signals like soil, including EXG, EXGR, GCI, GNDVI, MGRVI, MSAVI, NDRE, OSAVI, RE, RECI, SAVI, and TGI. All of them, including their standard deviations (std), were highly statistically significant with respect to construct and control differences, except for NDRE and RECI (mean and std), and standard deviation of NDVI, OSAVI, and RE. Tukey tests showed that trees containing the grape and poplar constructs trees were significantly different from each other for every remote sensing trait, with the exception of standard deviations of Blue, Green, Red, RE, DRE, SAVI, OSAVI, MSAVI, RECI, and means of TGI, GRVI, MGRVI, EXG, EXGR, NDRE, RECI, suggesting that these indexes are less suited for distinguishing leaves with different shades of purple. Means for the dark-leaved trees containing the grape construct were different from the green controls for all indexes, apart from Blue, Green ($P = 0.09$), Red, near-infrared (NIR) ($P = 0.06$), RE, MGRVI, EXG, EXGR, NDRE, GNDVI, GCI, and RECI, suggesting that these indexes are relatively poor parameters for comparing green to purple or dark-hue leaves. Overall, these results suggest that traditional indexes designed to compare "greenness" are insufficient for purple-colored plants. Indexes that incorporate NIR and infrared (IR) bands (such as ARI) will be needed if UAS evaluations are to serve as a robust proxy for traditional physiological assessments.

Shadow area—a two-dimensional proxy for canopy density that supplemented our LiDAR structural measurements—was nearly the same and not significantly different in trees containing the poplar construct compared with the control trees (−7%), but was highly significantly different between trees with the two constructs; it was 55% smaller in trees with the grape construct compared with the control trees (Table 1, Supplemental Table 1B). Trees with the poplar construct and control trees visually appeared the same in crown size in the field, and unsurprisingly—as detailed above—they showed no significant differences for height, diameter, or volume index traits (Supplemental Table 1).

Overall performance of the purple trees. Transgenic trees with an overexpressed MYB119 gene from *Populus trichocarpa* had moderately pigmentated and subjectively beautiful foliage. They had a low rate of instability among gene insertion events and did not differ significantly from controls for any growth trait, including crown volume inferred by shadow area (measured by remote sensing). They also did not show any evidence of frost or heat damage based on visual inspection in the field. This result is consistent with previous literature using the same construct in another poplar hybrid, *Populus alba* × *P. tremula* var. *glandulosa*; no significant differences were seen in height, diameter, or internode length compared with control trees after 2 months in a field trial (Cho et al. 2016). The leaf physiology traits were also very similar between the poplar construct and control trees; the only exceptions were some measures of leaf temperature, ETR, and conductance (Supplemental Table 1B). Under a hot and dry day, poplar construct trees had higher leaf temperatures and lower conductance but maintained higher photochemical efficiency. Overall, these differences resulted in minor and statistically nonsignificant changes in growth rate, survival, and crown volume during this multiyear study.

Our remote sensing analyses extended and supported results from our ground- and laboratory-based measurements of purple-colored trees. However, many of the indexes employed failed to provide useful information about the purple trees, especially those designed to measure "greenness." Presumably, indices incorporating NIR, RedEdge, and Thermal IR bands will be essential for robust UAS-based physiological assessments in pigmented cultivars. However, before such approaches can be used in place of ground-based phenotypic analysis, further studies are needed with a variety of tree phenotypes and field environments.

The trees transformed with an overexpressed copy of the *Vitis vinifera* MYBA1 gene, although having the same promoter as the poplar construct, exhibited very dark foliage and much reduced growth and survival. It also led to a high rate of instability of pigmentation. For reasons beyond the scope of this study, the grape-derived transcription factor clearly interacted with poplar biosynthetic machinery very differently from the poplar-derived gene. The negative effect of the grape transgene is consistent with prior studies looking at *Citrus aurantifolia* using the same construct; two transgenic lines showed intense pigmentation, curled leaves, and never grew beyond 15 cm in the greenhouse after 2 years (Dutt et al. 2016). Production of anthocyanins is a metabolically expensive process, and high levels of anthocyanins may be detrimental to plant growth (Bradley et al. 2002). In addition, their reduced stomatal conductance and photosynthetic activity may have led to reduced carbon uptake and elevated heat damage during warm periods. These trees are clearly maladapted to the Willamette Valley test environment.

By contrast, the trees containing the poplar construct appear well suited as an ornamental tree in western Oregon. It is nearly identical in performance to the controls over several years of study (and based on visual inspection also grew well though the 2025 growing season), but did not outgrow controls, suggesting a high degree of biosafety should it spread via pollen, seed, or vegetative means. Moreover, because trees will be vegetatively propagated, a variety of sterility approaches, including genetic disruption of genes essential for flowering by gene editing (e.g., Klocko et al. 2023; Nagle et al. 2023), could be employed to reduce negative perception of transgenes entering planted or wild gene pools (Strauss et al. 2017)—as well as to obviate the small risk that they might outcompete wild poplars. However, it has long been known that highly pigmented, anthocyanin-enriched foliar tissues, although favored in specific circumstances, species, and cell types for specific stress tolerance or other traits (Gould et al. 1995; Hughes and Lev-Yadun 2023), are rare both in nature and horticulture (Hawkins 2026). This is likely to be because they are generally inferior in health and productivity to green-leaved plants (Gould 2004). In *Populus*, nontransgenic cultivars of *Populus deltoides* with purple and red leaves have been studied previously, and the pigmented trees were shown to have reduced plant height, leaf number, ground diameter, and leaf area compared with a green-leafed variety (Xinghao et al. 2022). In sum, it is highly likely that use of poplars with constitutively pigmented leaves would have a neutral or net negative effect on plant fitness, thus would impose no significant threat for invasion of wild populations if used as a fertile ornamental plant.

References Cited

Bradley JM, Davies KM, Deroles SC, Bloor SJ, Lewis DH. 2002. The maize Lc regulatory gene up-regulates the flavonoid biosynthetic pathway of petunia. Plant J. 13(3):381–392. https://doi.org/10.1046/j.1365-313X.1998.00031.x.

Cappellini F, Marinelli A, Toccaceli M, Tonelli C, Petroni K. 2021. Anthocyanins: From mechanisms of regulation in plants to health benefits in foods. Front Plant Sci. 12:748049. https://doi.org/10.3389/fpls.2021.748049.

Chagné D, Lin-Wang K, Espley RV, Volz RK, How NM, Rouse S, Brendolise C, Carlisle CM, Kumar S, De Silva N, Micheletti D, McGhie T, Crowhurst RN, Storey RD, Velasco R, Hellens RP, Gardiner SE, Allan AC. 2013. Ancient duplication of apple MYB transcription factors is responsible for novel red fruit-flesh phenotypes. Plant Physiol. 161(1):225–239. https://doi.org/10.1104/pp.112.206771.

Cho J-S, Nguyen VP, Jeon H-W, Kim M-H, Eom SH, Lim YJ, Kim W-C, Park E-J, Choi Y-I, Ko J-H. 2016. Overexpression of PtrMYB119, a R2R3-MYB transcription factor from *Populus trichocarpa*, promotes anthocyanin production in hybrid poplar. Tree Physiol. 36(9):1162–1176. https://doi.org/10.1093/treephys/tpw046.

Dai F, Shi J, Yang C, Li Y, Zhao Y, Liu Z, An T, Li X, Yan P, Dong C. 2023. Detection of anthocyanin content in fresh Zijuan tea leaves based on hyperspectral imaging. Food Control. 152:109839. https://doi.org/10.1016/j.foodcont.2023.109839.

Daudet FA, Le Roux X, Sinoquet H, Adam B. 1999. Wind speed and leaf boundary layer conductance variation within tree crown: Consequences on leaf-to-atmosphere coupling and tree functions. Agric For Meteorol. 97(3):171–185. https://doi.org/10.1016/S0168-1923(99)00079-9.

Dutt M, Stanton D, Grosser JW. 2016. Ornacitrus: Development of genetically modified anthocyanin-expressing citrus with both ornamental and fresh fruit potential. J Am Soc Hortic Sci. 141(1):54–61. https://doi.org/10.21273/JASHS.141.1.54.

Fang H, Dong Y, Yue X, Hu J, Jiang S, Xu H, Wang Y, Su M, Zhang J, Zhang Z, Wang N, Chen X. 2019. The B-box zinc finger protein MdBBX20 integrates anthocyanin accumulation in response to ultraviolet radiation and low temperature. Plant Cell Environ. 42(7):2090–2104. https://doi.org/10.1111/pce.13552.

Filichkin SA, Meilan R, Busov VB, Ma C, Brunner AM, Strauss SH. 2006. Alcohol-inducible gene expression in transgenic *Populus*. Plant Cell Rep. 25(7):660–667. https://doi.org/10.1007/s00299-005-0112-3.

Gitelson AA, Merzlyak MN, Chivkunova OB. 2001. Optical properties and nondestructive estimation of anthocyanin content in plant leaves. Photochem Photobiol. 74(1):38–45. https://doi.org/10.1562/0031-8655(2001)0740038OPANEO2.0.CO2.

Gould KS. 2004. Nature's Swiss Army Knife: The diverse protective roles of anthocyanins in leaves. J Biomed Biotechnol. 2004(5):314–320. https://doi.org/10.1155/S1110724304406147.

Gould KS, Kuhn DN, Lee DW, Oberbauer SF. 1995. Why leaves are sometimes red. Nature. 378(6554):241–242. https://doi.org/10.1038/378241b0.

Gu X, Cai W, Fan Y, Ma Y, Zhao X, Zhang C. 2018. Estimating foliar anthocyanin content of purple corn via hyperspectral model. Food Sci Nutr. 6(3):572–578. https://doi.org/10.1002/fsn3.588.

Hawkins L. 2026. Colored and variegated broad-leaved trees and shrubs. Pacific Horticulture. https://pacifichorticulture.org/articles/colored-and-variegated-broad-leaved-trees-and-shrubs/.

Hobbs SLA, Warkentin TD, DeLong CMO. 1993. Transgene copy number can be positively or negatively associated with transgene expression. Plant Mol Biol. 21(1):17–26. https://doi.org/10.1007/BF00039614.

Hughes NM, Burkey KO, Cavender-Bares J, Smith WK. 2012. Xanthophyll cycle pigment and antioxidant profiles of winter-red (anthocyanic) and winter-green (acyanic) angiosperm evergreen species. J Exp Bot. 63(5):1895–1905. https://doi.org/10.1093/jxb/err362.

Hughes NM, Lev-Yadun S. 2023. Review: Why do some plants have leaves with red or purple undersides? Environ Exp Bot. 205:105126. https://doi.org/10.1016/j.envexpbot.2022.105126.

Kim C, van Iersel MW. 2023. Image-based phenotyping to estimate anthocyanin concentrations in lettuce. Front Plant Sci. 14:1155722. https://doi.org/10.3389/fpls.2023.1155722.

Klocko AL, Elorriaga E, Ma C, Strauss SH. 2023. Variation in floral form of CRISPR knock-outs of the poplar homologs of LEAFY and AGAMOUS after FT heat-induced early flowering. Hortic Res. 10(8):uhad132. https://doi.org/10.1093/hr/uhad132.

Kramer PJ, Kozlowski TT. 1979. Physiology of woody plants. Academic Press, Inc., London, UK.

Kumar S, Fladung M. 2001. Gene stability in transgenic aspen (*Populus*). II. Molecular characterization of variable expression of transgene in wild and hybrid aspen. Planta. 213(5):731–740. https://doi.org/10.1007/s004250100535.

Marshall B, Biscoe PV. 1980. A model for C3 leaves describing the dependence of net photosynthesis on irradiance. J Exp Bot. 31(1):29–39. https://doi.org/10.1093/jxb/31.1.29.

Martin C, Butelli E. 2025. The purple tomato story; from laboratory bench to the consumer. ACS Food Sci Technol. 5(1):19–28. https://doi.org/10.1021/acsfoodscitech.4c00692.

Meilan R, Ma C. 2006. Poplar (*Populus* spp.), p 143–151. In: Wang K (ed). Agrobacterium protocols volume 2. Humana Press. https://doi.org/10.1385/1-59745-131-2:143.

Nagle MF, Nahata SS, Zahl B, Niño de Rivera A, Tacker XV, Elorriaga E, Ma C, Goralogia GS, Klocko AL, Gordon M, Joshi S, Strauss SH. 2023. Knockout of floral and meiosis genes using CRISPR/Cas9 produces male-sterility in Eucalyptus without impacts on vegetative growth. Plant Direct. 7(7):e507. https://doi.org/10.1002/pld3.507.

National Weather Service. 2026. Hourly weather observations for KCVO. National Oceanic and Atmospheric Administration. https://www.weather.gov/wrh/timeseries?site=KCVO&hourly=true.

Okitsu N, Noda N, Chandler S, Tanaka Y. 2018. Flower color and its engineering by genetic modification, p 29–62. In: Van Huylenbroeck J (ed). Ornamental crops. Springer International Publishing, Cham, Switzerland. https://doi.org/10.1007/978-3-319-90698-0_3.

Stinziano J, Roback C, Sargent D, Murphy B, Hudson P, Muir C. 2019. Photosynthesis: Tools for plant ecophysiology & modeling. 2.1.5. https://CRAN.R-project.org/package=photosynthesis.

Strauss SH, Jones KN, Lu H, Petit JD, Klocko AL, Betts MG, Brosi BJ, Fletcher RJ Jr, Needham MD. 2017. Reproductive modification in forest plantations: Impacts on biodiversity and society. New Phytol. 213(3):1000–1021. https://doi.org/10.1111/nph.14374.

van den Berg AK, Perkins TD. 2005. Nondestructive estimation of anthocyanin content in autumn sugar maple leaves. HortScience. 40(3):685–686. https://doi.org/10.21273/HORTSCI.40.3.685.

Xinghao C, Hanqi LIU, Xinjian Z, Xiangjun C, Minsheng Y, Jun Z. 2022. Comparative analysis of photosynthetic and physiological characteristics of red-leafed 'Quanhong' and 'Xuanhong' poplar cultivars. Acta Hortic Sin. 49(2):437. https://doi.org/10.16420/j.issn.0513-353x.2020-0759.

Zhao D, Tao J. 2015. Recent advances on the development and regulation of flower color in ornamental plants. Front Plant Sci. 6:261. https://doi.org/10.3389/fpls.2015.00261.

Zhao S, Blum JA, Ma F, Wang Y, Borejsza-Wysocka E, Ma F, Cheng L, Li P. 2022. Anthocyanin accumulation provides protection against high light stress while reducing photosynthesis in apple leaves. Int J Mol Sci. 23(20):12616. https://doi.org/10.3390/ijms232012616.